Crystallographic study of $LaNi_{5-x}Sn_x$ ($0.2 \leq x \leq 0.5$) compounds and their hydrides

J.-M. Joubert[a,*], M. Latroche[a], R. Cerny[b], R.C. Bowman, Jr.[c], A. Percheron-Guégan[a], K. Yvon[b]

[a]*Laboratoire de Chimie Métallurgique des Terres Rares, 2-8 rue Henri Dunant, 94320 Thiais Cedex, France*

[b]*Laboratoire de Cristallographie, Université de Genève, 24 Quai E. Ansermet, 1211 Genève 4, Switzerland*

[c]*Jet Propulsion Laboratory, California Institute of Technology, Pasadena, California 91109, USA*

Abstract

The structural properties of tin substituted $LaNi_5$ compounds and corresponding deuterides have been investigated by single crystal X-ray and neutron powder diffraction. Tin is found to substitute nickel exclusively on site 3*g* of space group P6/*mmm*. No other significant disorder occurs in the structure. At tin contents of x=0.4 and x=0.5, the crystal structures of the deuterides do not significantly deviate from those of other metal substituted $LaNi_5$ deuterides. At a tin content of x=0.2, with higher deuterium content, however, a symmetry decrease to non-centrosymmetric space group P6*mm* is observed due to partial deuterium ordering.

Keywords : Sn, AB_5, hydrides, neutron diffraction, single crystal diffraction

* corresponding author. E-mail : joubert@glvt-cnrs.fr

1. Introduction

$LaNi_5$ and most of its substitutional derivatives, after very few absorption-desorption hydrogen cycles, suffer from loss of their crystallinity evidenced by large diffraction line broadening [1]. With further cycling, the phenomenon is accentuated and leads to disproportionation [2] of the alloys and decrease of the storage capacity [3,4]. Few substituted compounds (e.g. aluminium substituted [1,5]) have the ability to better retain the crystallinity. Among them, tin substituted compounds have especially attracting properties because they show no line broadening and little capacity decay even after 10000 cycles [4].

The mechanisms for such behaviour have not yet been elucidated. Goodell has formulated a hypothesis [5] for aluminium substitution. The substitution of nickel by larger atoms on site 3*g* (space group P6/*mmm*) is supposed to prevent a possible La/Ni exchange which would be responsible for the broadening. Therefore determining on which of the two available nickel sites (2*c* or 3*g*) tin substitutes is important.

Contradictory results have been obtained concerning the crystal structure of tin substituted compounds. Wasz et al. [6] have made Rietveld refinement of X-ray powder diagrams and states a preferential occupation of site 3*g* by tin but no quantitative results are given. As the alloys were synthesised by mechanical alloying of $LaNi_5$ with tin and as no analytical results on sample compositions are given, doubts exist concerning the equilibrium state and the stoichiometry of the compounds obtained (compounds are probably over-stoichiometric in nickel).

In addition, Hughes et al. [7] have interpreted unexpectedly large anisotropic displacement parameters in an X-ray single crystal investigation of $LaNi_{4.6}Sn_{0.4}$ compounds by positional disorder of La and Ni on site 2*c*. Again no definite results were given and the model was presented as a simple hypothesis.

The aim of this work was to determine conclusively the crystal structure of the tin substituted intermetallic compounds. In a second step, the crystal structure of the hydrides (deuterides) have been obtained in order to make a comparison with the other structures known for substituted $LaNi_5$ compounds and find whether or not a different hydrogen distribution could be associated with the peculiar properties of the tin compounds.

2. Experimental

The $LaNi_{5-x}Sn_x$ alloys were prepared following the procedure described in [8]. They were synthesised at the Ames Laboratory of the Iowa State University (x=0.2) or at Hydrogen Components, Inc. (x=0.4, 0.5) by arc-melting the pure elements. The as-cast ingots were then annealed at 950°C for 120 h (x=0.2) or 91 h (x=0.4, 0.5). Metallographic examination and elemental analysis by electron probe micro-analysis (EPMA) were performed to check the homogeneity of the alloys. P-c-T curves were measured using the Sievert's method. Neutron diffraction patterns were recorded on the 3T2 instrument at the Laboratoire Léon Brillouin in Saclay (France). Experiments were carried out on powdered intermetallic compounds in a neutron-transparent vanadium container. The batches of alloy were subsequently activated by 5 absorption-desorption deuterium cycles, transferred to a silica tube for the last deuterium absorption and closed under controlled pressure after accurate measurement of deuterium content to obtain the neutron diffraction patterns for the deuterides. All the patterns were refined with the Rietveld method using FULLPROF [9].

Small parallelepiped single crystals (typical larger dimension 60 μm) were found in the crushed alloy. The diffraction measurement were performed on a Philips PW1100 four-circle diffractometer with Mo K_α radiation in theta range 0°-30°. Half of the reciprocal space was measured in this region and equivalent reflections were averaged. Analytical absorption correction was made from the measured crystal shape (indexed faces) and size. Refinements were made using XTAL 3.2 [10].

3. Results

The matrix compositions of $LaNi_{5-x}Sn_x$ alloys (x=0.2, 0.4, 0.5) are homogeneous and close to the nominal ones as can be checked in Table 1. For x=0.4 and x=0.5, inclusions were found whose composition is close to a LaNiSn phase. The presence of small amount of this phase (1 wt % and 2 wt %) with $SiCo_2$ structure type was confirmed by X-ray diffraction.

The P-c-T curves measured at 25°C are plotted in Fig. 1 together with data for $LaNi_5$ (x=0). One can notice the lowering of the plateau pressure and the decrease of hydrogen capacity as a function of increasing tin content. The P-c-T curve obtained for x=0.2 is in excellent agreement with that measured by Luo et al. [11].

The results of the Rietveld refinement of the neutron diffraction patterns are summarized in Table 2. The three tin substituted compounds were fitted as substitutional derivatives of $LaNi_5$ in space group P6/*mmm* (La on 1*a* (0,0,0); Ni on 2*c* (1/3,2/3,0) and 3*g* (1/2,0,1/2)). For the refinement and to minimize correlations between the different parameters, the total tin content was fixed to the nominal content in agreement with EPMA results. After verification that the substitution of lanthanum by tin led to poorer refinements, tin was assumed to substitute exclusively on the two nickel sublattices, and its distribution on sites 2*c* and 3*g* was refined. In addition, one displacement parameter per site was considered and refined as isotropic. For x=0.5, the impurity phase LaNiSn with $SiCo_2$ structure type [12] was taken into account in the refinement.

The results of X-ray single crystal diffraction are given in Table 3. Here the total tin occupancies were left unconstrained, yielding overall tin contents for the three crystals (x=0.19, 0.45 and 0.52) close to the respective nominal values. Anisotropic displacement parameters were refined for each site and are given in Table 4 together with the corresponding calculated equivalent isotropic parameters.

The crystal structures of the deuterides have been investigated by Rietveld refinement of the neutron powder diffraction data. In each case, the overall metal substructure of $LaNi_5$ is retained. Tin was assumed to keep the same distribution on sites 2*c* and 3*g* as found for intermetallic compounds and not further refined. For x=0.5 and x=0.4, deuterium occupies the same four interstitial sites of space group P6/*mmm* as those in most other metal substituted $LaNi_5$ compounds for deuterium contents between 5 and 6 D per formula unit : 4*h* (1/3, 2/3, z≈0.38), 6*m* (x≈0.14, 2x, 1/2), 12*n* (x≈0.47, 0, z≈0.11), 12*o* (x≈0.21, 2x, z≈0.33) [13,14]. The refined occupancy factors are given in Table 5. Total refined deuterium contents are in agreement with compositions measured by Sievert's method during the loading of the deuterides. On the contrary, for x=0.2, the refinement of the P6/*mmm* model lead to a deuterium composition far below the measured composition (4.9 D/f.u. instead of 6.1 D/f.u.). By comparison with what is observed in

$LaNi_5$-D system, various models were tried following the work of Lartigue et al. [15]. As no superstructure peak indicating the doubling of the cell was observed, the $CaCu_5$ cell was conserved. However, to take into account the possible ordering of deuterium atoms, the symmetry was decreased to P6*mm* which lead to a splitting of three of the four deuterium sites as indicated in Table 5. The refinement of non-constrained occupancies of those sites shows in each case the preferential occupation of one of the two sites. To keep the number of refined parameters reasonable, the atomic positions were refined but kept constrained by the pseudo-mirror symmetry (i.e. it was assumed that the symmetry decrease is only due to difference in occupancy factors of split sites and not in positional variations). Significant improvement of R_{Bragg} factor (4.4% instead of 6.7%) is observed and the total refined deuterium content (6.2 D/f.u.) is now in agreement with the measured value. In Fig. 2, the deuterium occupancy factors are plotted as a function of tin composition.

4. Discussion

Cell parameters increase linearly with tin substitution (x) in $LaNi_5$ in agreement with the replacement of nickel (R_{Ni}=1.24 Å) by a larger atom (R_{Sn}=1.62 Å). Due to this difference in size, the substitution seems to be limited to x=0.5 where a significant amount of secondary phase is found to precipitate. Cell volumes are in excellent agreement with those found by Luo et al. [8]. A linear decrease of the logarithmic plateau pressure at 25°C accompanies the cell volume increase as was found at 100°C in this system [8] and as is generally observed in other substitution systems of $LaNi_5$. Decrease of the hydrogen capacity as a function of x is observed.

The crystal structure of the intermetallic substituted compounds with respect to the location of tin atoms on the two possible nickel sites has been investigated by powder neutron diffraction and single crystal X-ray diffraction. From powder neutron diffraction, with no doubts and at any composition, tin appears to substitute exclusively on site 3*g*. This result is confirmed by single crystal diffraction refinement for which occupancies of site 2*c* are not significant and is in agreement with the trend for large atoms to substitute preferentially on this site where there is more space to fit them [1].

Problems with anisotropic displacement parameters possibly related to positional disorder were previously reported from X-ray single crystal diffraction experiments [7]. In our analyses, as far as can be observed in Table 4, only a small anisotropy appears, lanthanum displacement ellipsoid being elongated along the c axis. Such anisotropic factors (U_{33} is 2-3 times U_{11}) are commonly observed in inorganic crystal structure and more particularly with intermetallic compounds without any questioning about the disorder. Those results have no common order with what was previously reported [7] (U_{33} up to 6 times U_{11} for La, U_{11} up to 10 times U_{33} for Ni_{2c}) indicating inconsistencies in this paper. From our results, there is no reason to invalidate the $CaCu_5$ model for those compounds. Finally, comparison can be made between the equivalent displacement factors obtained by X-ray single crystal analysis with the values obtained from neutron powder diffraction. The two techniques investigate two different kinds of particles (electrons and nuclei). Therefore, the excellent agreement between displacement factors testifies the quality of our model.

The crystal structure of the deuterides formed by $LaNi_{5-x}Sn_x$ (x=0.2, 0.4, 0.5) alloys was investigated for the first time. For x=0.4 and x=0.5, the model refined is in agreement with previous studies on substituted $LaNi_5$ deuterides [14]. Occupancy factors were refined and values obtained for the different sites correspond to what is generally observed in such systems. The decrease of capacity with x value is explained by the smaller occupancy of each site as summarized in Fig 2.

For x=0.2, the refinement clearly shows that the P6/*mmm* model is wrong. In the work of Lartigue et al. [15] in which $LaNi_5$ deuterides are investigated as a function of composition, two different kinds of ordering were taken into account :

- for low deuterium composition ($LaNi_5D_{5.0}$) : decrease of symmetry from P6/*mmm* to P6*mm* (keeping the same cell) due to ordering of deuterium atoms was considered : site 4*h* splits into two sites 2*b*, 12*n* into two 6*d*, 12*o* into two 6*e*, 6*m* is conserved in 6*e*. For each of the split sites, only the occupancy of one site per pair was considered, the other occupancy being fixed to 0. Finally, the authors could not choose between this P6*mm* model and the classical P6/*mmm* model.

- for high deuterium composition ($LaNi_5D_{6.7}$) : a superstructure peak was observed indicating a doubling of the cell along the c-axis. In addition to the ordering described for

$LaNi_5D_{5.0}$ (exclusion of 14 sites per $LaNi_5$ unit), further splitting of the remaining sites occurs for which occupancy factors are related by an order parameter α. Space group becomes $P6_3mc$.

Following this work, considering the low tin content which makes the compound close to $LaNi_5$ and high deuterium content, it was assumed that a symmetry decrease could occur for $LaNi_{4.8}Sn_{0.2}D_{6.1}$ sample. As no superstructure peak was observed in our pattern, only ordering of the P6*mm* model was considered. Contrary to what was tried by Lartigue et al. and to clearly decide between the P6*mm* and P6/*mmm* model, the occupancy factors of all the split sites were refined in P6*mm* model. Similar occupancies for each corresponding site (e.g. 2*b*(1) (1/3,2/3,0.38) and 2*b*(2) (1/3,2/3,0.62) which derive from the 4*h* (1/3,2/3,0.32)) would have indicated that P6/*mmm* was correct. On the contrary, occupancy of one site and total rejection of the other would have corresponded to the P6*mm* model as refined by Lartigue et al. The results obtained in this work clearly shows the ordering of deuterium atoms. However, it appears that the sites which were not considered in the case of $LaNi_5$ are not completely empty.

5. Conclusions

The crystal structures of three $LaNi_{5-x}Sn_x$ compounds and their deuterides have been investigated by single crystal X-ray and powder neutron diffraction. Concerning the intermetallic compounds and for each composition, the P6/*mmm* $CaCu_5$ model is definitively confirmed and no particular structural disorder is evidenced. Tin substitutes only for nickel and is exclusively located on site 3*g*. For x=0.4 and x=0.5, the deuterium locations and occupancies agree with what is generally observed for other substituted compounds deuterides. On the contrary, for x=0.2, ordering of deuterium is observed leading to a symmetry decrease in the $CaCu_5$ cell. Similar behaviour was already observed for $LaNi_5$ deuterides. As $LaNi_5$ itself has poor solid-gas cycling properties, the peculiar capacity of tin substituted compounds to conserve good crystallinity after extensive cycling can not be explained by unusual structural features of the deuterides. Therefore, it seems that only the presence of a large substituted atom in site 3*g*, like in the case of aluminium [5] is responsible for this behaviour. The exact mechanism for degradation and role of those large atoms need still to be further investigated.

Acknowledgements

The authors wish to thank Mrs F. Demany, Mrs F. Briaucourt and Mr L. Touron for technical assistance and F. Bourée-Vigneron for the neutron diffraction experiments. This research was partially supported by the United States Department of Energy under Grant DE-FG03-94ER14493. to Caltech The Jet Propulsion Laboratory is operated by the California Institute of Technology under contract with the U.S. National Aeronautics and Space Administration.

References

[1] A. Percheron-Guégan, C. Lartigue, J.-C. Achard, P. Germi and F. Tasset, *J. Less-Common Met.*, 74 (1980) 1-12.

[2] R.C. Bowman, Jr., C.H. Luo, C.C. Ahn, C.K. Witham and B. Fultz, *J. Alloys Comp.*, 217 (1995) 185-192

[3] Y. Josephy, E. Bershadsky and M. Ron, *J. Less-Common Met.*, 172-174 (1991) 997-1008.

[4] S.W. Lambert, D. Chandra, W.N. Cathey, F.E. Lynch and R.C. Bowman, Jr., *J. Alloys Comp.*, 187 (1992) 113-135.

[5] P.D. Goodell, *J. Less-Common Met.*, 99 (1984) 1-14.

[6] M.L. Wasz, P.B. Desch and R.B. Schwarz, *Phil. Mag.*, A74 (1) (1996) 15-22.

[7] J.M. Hughes, J.S. Cantrell and R.C. Bowman, Jr., *Int. J. Hydrogen Energy*, 22 (2/3) (1997) 347-349.

[8] S. Luo, J.D. Clewley, T.B. Flanagan, R.C. Bowman, Jr., and L.A. Wade , *J. Alloys Comp.*, 267 (1998) 171-181.

[9] J. Rodriguez-Carvajal, *Abstract of the Satellite Meeting on Powder Diffraction*, Congr. Int. Union of Crystallography, Toulouse, France, 1990, p. 127.

[10] S.R. Hall, H.D. Flack and J.M. Stewart, Eds. (1992). XTAL 3.2 Reference Manual. Universities of Western Australia, Geneva and Maryland, Lamb : Perth.

[11] S. Luo, W. Luo, J.D. Clewley, T.B. Flanagan and R.C. Bowman, Jr., *J. Alloys Comp.*, 231 (1995) 473-478.

[12] J.L.C. Daams and K.H.J. Buschow, *Philips J. Res.*, 39(3) (1984) 77-81.

[13] A. Percheron-Guégan, C. Lartigue and J.-C. Achard, *J. Less-Common Met.*, 109 (1985) 287-309.

[14] M. Latroche, J. Rodriguez-Carvajal, A. Percheron-Guégan and F. Bourée-Vigneron, *J. Alloys Comp.*, 218 (1995) 64-72.

[15] C. Lartigue, A. Percheron-Guégan, J.-C. Achard and J.-L. Soubeyroux, *J. Less-Common Met.*, 113 (1985) 127-148.

Table caption

Table 1 : Compositional analysis of the alloys by EPMA

Table 2 : Results of the neutron diffraction Rietveld refinement for the intermetallic compounds $LaNi_{5-x}Sn_x$ (space group P6/*mmm*). Lattice parameters, tin occupancies, displacement parameters for each site, goodness of fit and intensity agreement factor are given for each composition.

Table 3 : $LaNi_{5-x}Sn_x$ X-ray single crystal results (space group P6/*mmm*) (agreement factors, min/max transmission factors and tin occupancies).

Table 4 : $LaNi_{5-x}Sn_x$ single crystal results (space group P6/*mmm*) (anisotropic displacement factors in $Å^2$ ($U_{13}=U_{23}=0$), equivalent isotropic factor U_{eq} and corresponding B value).

Table 5 : Results of the neutron diffraction experiments on $LaNi_{5-x}Sn_x$ deuterides. Deuterium composition from Sievert's method measurement, space group, lattice parameters, cell volume and expansion as regard to the intermetallic compound, displacement factors (one only refined for all the deuterium atoms), deuterium occupancies (in atoms per formula unit), total refined D content and agreement factors are given.

Figure caption

Fig. 1 : P-c-T curves at 25°C for $LaNi_{5-x}Sn_x$ compounds.

Fig. 2 : Deuterium occupancy factors as a function of tin composition in $LaNi_{5-x}Sn_x$ deuterides.

Alloy (nominal)	Composition	Inclusions (wt %)
$LaNi_{4.8}Sn_{0.2}$	$La_{0.99(1)}Ni_{4.80(3)}Sn_{0.21(3)}$	-
$LaNi_{4.6}Sn_{0.4}$	$La_{1.01(1)}Ni_{4.61(2)}Sn_{0.38(2)}$	$La_{0.98}Ni_{1.01}Sn_{1.01}$ (1%)
$LaNi_{4.5}Sn_{0.5}$	$La_{1.01(1)}Ni_{4.51(1)}Sn_{0.48(1)}$	$La_{0.98}Ni_{1.02}Sn_{1.01}$ (2%)

Table 1 : Compositional analysis of the alloys by EPMA

x	0.2	0.4	0.5
a (Å)	5.051(1)	5.088(1)	5.104(1)
c (Å)	4.020(1)	4.055(1)	4.074(1)
V (Å^3)	88.81	90.90	91.92
Sn 2*c* (atom/f.u.)	-0.005(13)	-0.013(16)	-0.016(16)
Sn 3*g* (atom/f.u.)	0.205(13)	0.413(16)	0.516(16)
B_{1a} (Å^2)	1.08(2)	1.03(2)	1.27(3)
B_{2c} (Å^2)	1.03(2)	0.94(2)	1.17(2)
B_{3g} (Å^2)	0.79(2)	0.61(1)	0.78(2)
χ^2	5.1	5.4	6.8
R_{Bragg} (%)	4.8	5.4	4.8

Table 2 : Results of the neutron diffraction Rietveld refinement for the intermetallic compounds $LaNi_{5-x}Sn_x$ (space group P6/*mmm*). Lattice parameters, tin occupancies, displacement parameters for each site, goodness of fit and intensity agreement factor are given for each composition.

x	0.2	0.4	0.5
R_{F2} (%)	3.9	3.2	4.4
Goodness of fit	1.3	1.7	1.3
Min/Max transmission	0.34/0.42	0.33/0.46	0.49/0.75
Largest unassigned densities (e/Å^3)	2.1	1.1	1.8
Sn 2*c* (atom/f.u.)	0.02(4)	0.07(1)	0.06(2)
Sn 3*g* (atom/f.u.)	0.14(2)	0.38(1)	0.46(2)
Total Sn (atom/f.u.)	0.16(6)	0.45(2)	0.52(4)

Table 3 : $LaNi_{5-x}Sn_x$ X-ray single crystal results (space group P6/*mmm*) (agreement factors, min/max transmission factors and tin occupancies).

	U_{11}	U_{22}	U_{33}	U_{12}	U_{eq}	$B_{eq}=8\pi^2U_{eq}$
x=0.2						
1*a*	$2U_{12}$	$2U_{12}$	0.0187(6)	0.0032(2)	0.0105(3)	0.83(2)
2*c*	$2U_{12}$	$2U_{12}$	0.0089(8)	0.0064(4)	0.0114(5)	0.90(4)
3*g*	0.0068(5)	$2U_{12}$	0.0087(5)	0.0022(3)	0.0069(4)	0.54(3)
x=0.4						
1*a*	$2U_{12}$	$2U_{12}$	0.0218(2)	0.0045(1)	0.0133(1)	1.05(1)
2*c*	$2U_{12}$	$2U_{12}$	0.0078(3)	0.0077(1)	0.0129(2)	1.02(1)
3*g*	0.0093(2)	$2U_{12}$	0.0068(2)	0.0035(1)	0.0079(1)	0.62(1)
x=0.5						
1*a*	$2U_{12}$	$2U_{12}$	0.0251(5)	0.0043(2)	0.0141(3)	1.11(2)
2*c*	$2U_{12}$	$2U_{12}$	0.0098(6)	0.0074(2)	0.0131(4)	1.03(3)
3*g*	0.0086(4)	$2U_{12}$	0.0076(4)	0.0030(2)	0.0077(3)	0.61(2)

Table 4 : $LaNi_{5-x}Sn_x$ single crystal results (space group P6/*mmm*) (anisotropic displacement factors in Å^2 ($U_{13}=U_{23}=0$), equivalent isotropic factor U_{eq} and corresponding B value).

Intermetallic composition	$LaNi_{4.8}Sn_{0.2}$		$LaNi_{4.6}Sn_{0.4}$	$LaNi_{4.5}Sn_{0.5}$
D composition (deuterium pressure (bar))	6.1 (7.2)		5.8 (6.7)	5.2 (5.1)
Space Group	P6*mm*		P6/*mmm*	P6/*mmm*
a (Å)	5.399(1)		5.392(1)	5.390
c (Å)	4.307(1)		4.313(1)	4.317
V (Å^3) (ΔV/V(%))	108.7(1) (+ 22.2%)		108.6 (+ 19.6%)	108.6(1) (+ 18.5%)
B_{1a}	1.53(5)	B_{1a}	1.14(3)	1.29(3)
B_{2b}	1.70(3)	B_{2c}	1.34(2)	1.48(2)
B_{3c}	1.41(2)	B_{3g}	1.14(1)	1.25(2)
D 2*b*(1) (1/3,2/3,0.38)	-0.07(3)	D 4*h* (1/3,2/3,0.38)	0.26(1)	0.21(1)
D 2*b*(2) (1/3,2/3,0.62)	0.55(3)			
D 6*e* (0.14,2x,0.5)	1.94(3)	D 6*m* (0.14,2x,1/2)	1.88(2)	1.78(3)
D 6*d*(1) (0.47,0,0.11)	2.65(5)	D 12*n* (0.47,0,0.11)	2.68(2)	2.61(3)
D 6*d*(2) (0.47,0,0.89)	0.13(2)			
D 6*e*(1) (0.21,2x,0.34)	0.16(4)	D 12*o* (0.21,2x,0.33)	0.69(2)	0.56(2)
D 6*e*(2) (0.21,2x,0.66)	0.73(5)			
Total D refined	6.2(3)		5.51(7)	5.15(9)
B_D (Å^2)	2.00(7)		1.82(6)	1.93(7)
χ^2	8.6		3.6	6.7
R_{Bragg}	4.4		4.3	5.5

Table 5 : Results of the neutron diffraction experiments on $LaNi_{5-x}Sn_x$ deuterides.

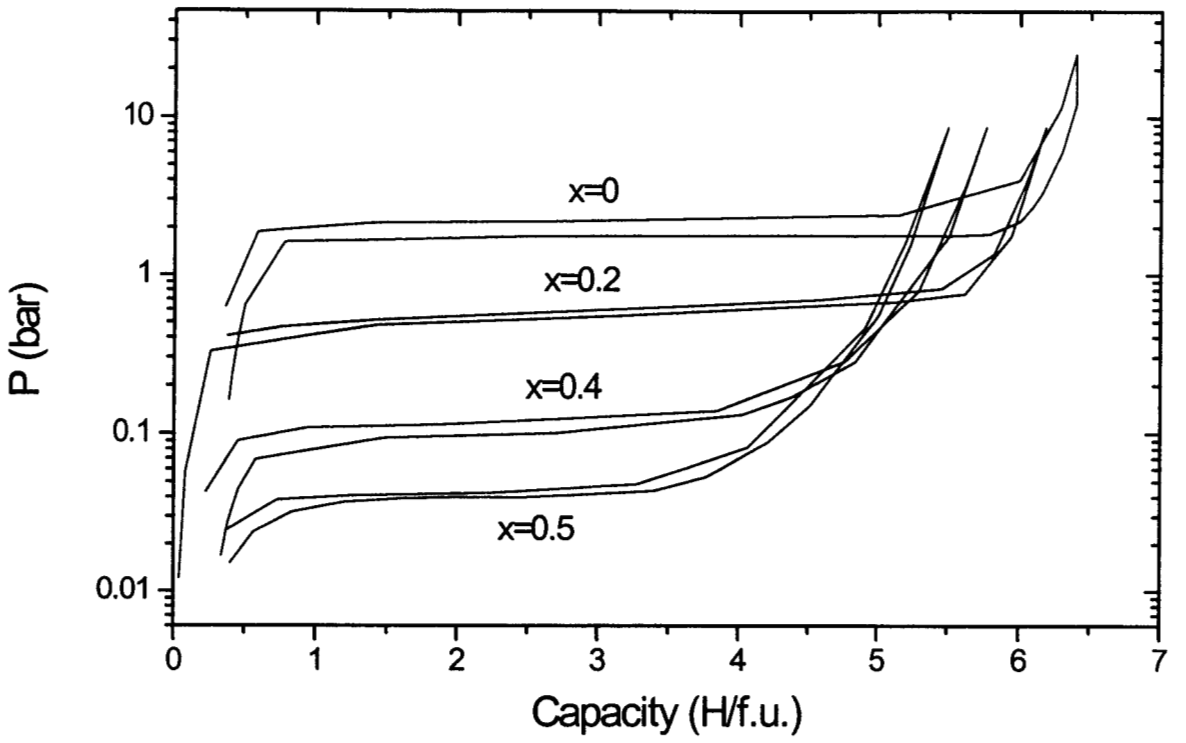

Fig. 1 : P-c-T curves at 25°C for $LaNi_{5-x}Sn_x$ compounds.

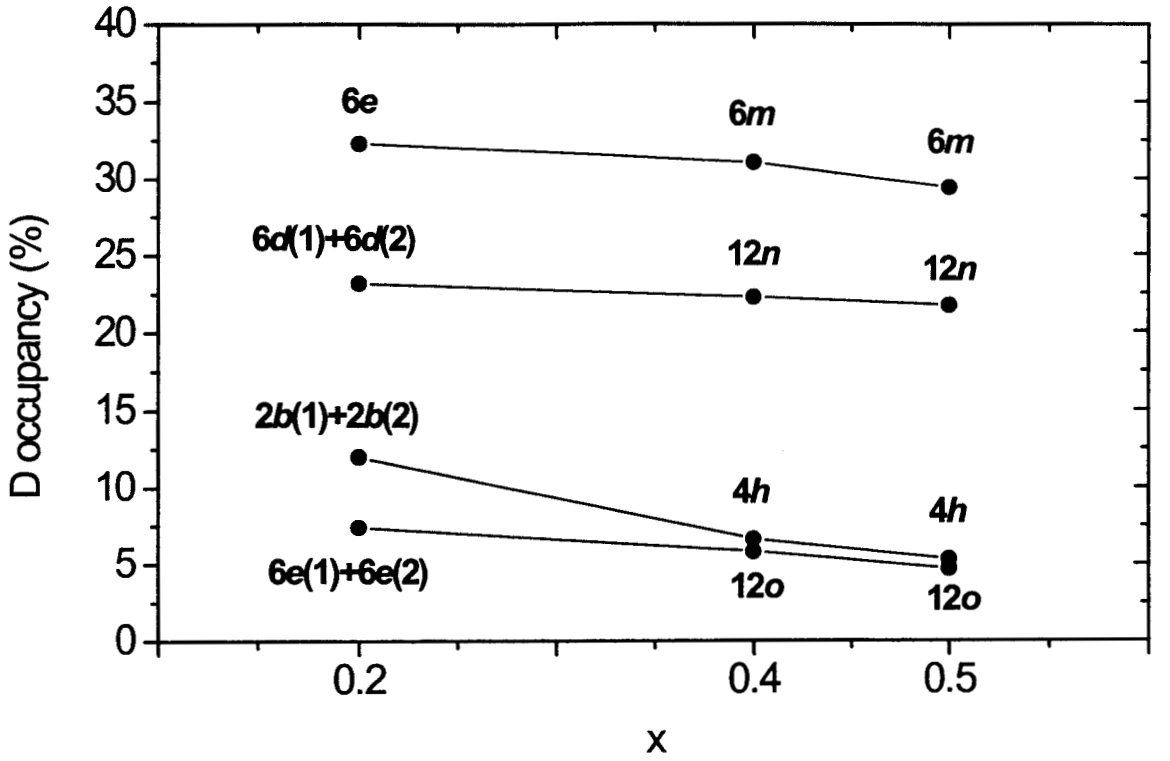

Fig. 2 : Deuterium occupancy factors as a function of tin composition in $LaNi_{5-x}Sn_x$ deuterides.